Gas orbits in a spiral potential

Gilberto C. Gómez[1] and Marco A. Martos[2]

[1] Centro de Radioastronomía y Astrofísica - Universidad Nacional Autónoma de México
Apartado Postal 3-72 (Xangari), Morelia, Mich. 58089, México
g.gomez@astrosmo.unam.mx
[2] Instituto de Astronomía - Universidad Nacional Autónoma de México
Apartado Postal 70-264, Ciudad Universitaria, D.F. 04510, México
marco@astroscu.unam.mx

Summary. We performed MHD simulations of the response of a gaseous galactic disk to a spiral perturbation in the background potential. In this poster, as a complement to M. Martos oral presentation, we present the results of our analysis of the gas flow and its interaction with the resonances expected from stellar orbit theory.

1 INTRODUCTION

In a previous work [1] it was shown that the response of a gaseous disk to a rotating 2-armed spiral potential representing the potential of the Milky Way is 4-armed beyond a certain distance. The axisymmetric part of that model included a disk, a bulge and a DM halo [2]. This is qualitatively consistent with the conventional picture for the spiral arms in our Galaxy, usually traced by HII regions. In a study of the self-consistency of the stellar disk to the imposed spiral perturbation [3], it was found that the stellar component was not in phase with the spiral beyond the 4:1 resonance, as predicted by [4, 5], using a similar model of non-axisymmetric perturbation plus a background potential (see also references within [3]). In the observational study of Drimmel and Spergel [6], the gas spiral extends up to corotation, again in consistency with the weak case in [4].

In this work, the study presented in [1] is extended to the MHD regime, complementing the analysis with the calculation of the gaseous orbits (in a Lagrangian sense) in order to compare them with the corresponding stellar orbits.

2 THE SIMULATIONS

The simulations were set up with an isothermal gaseous disk at 8000 °K in rotational equilibrium in the axisymmetric background potential [2] taking

into account the centrifugal force, (thermal + magnetic) pressure gradient and magnetic tension. The gas density followed an exponential law with a 15 kpc scale length. The magnetic field was purely azimuthal in the beginning (although it rapidly adopted a spiral geometry), with a strength of 2μG at the solar circle (at 8.5 kpc) and an exponential decay with a 25 kpc scale length.

This equilibrium was perturbed by a two arm spiral [3] with a pitch angle of $15.5^{\rm o}$, imposed as a fixed background potential with an amplitude such that the radial force (averaged over the radial extent) is 2% the axisymmetric background force. This spiral perturbation rotates with a pattern speed $\Omega_P = 25\,{\rm km\ s^{-1}\,kpc^{-1}}$, which places the inner Lindblad, 4:1, -4:1 and outer Lindblad resonance radii at 2.42, 5.38, 11.69 and 14.41 kpc, respectively. The corotation radius is at 8.80 kpc. A variety of values for the arm strength, magnetic field intensity, gas temperature, and pattern speed were tested.

The full MHD simulations were performed with the ZEUS code [7, 8] on a 2D grid in cylindrical geometry. The numerical grid extended from 1 kpc through 18 kpc in radius and a full circle in azimuth, with 512×1024 grid points. All cases were solved in the pattern reference frame in order to avoid smearing due to numerical diffusion. No self gravity of the gas was considered, although we plan to add it in a forthcoming paper.

Very rapidly (less than 200 Myr), the gas reacts to the perturbation developing two $14^{\rm o}$-pitch spiral arms in the internal region, up to the inner Lindblad resonance (ILR). Just outside this resonance, these arms break (at which point a spur is formed), but can be traced further out (with a $9^{\rm o}$ pitch angle), until just outside the 4:1 resonance. Also, a second pair of arms develops (with a $13^{\rm o}$ pitch) spanning from just outside the ILR, across the 4:1 resonance, until just before corotation (although a very weak extension can be traced outside corotation almost to the outer Lindblad resonance). This behavior is somewhat different in several details from that reported by [9] and it will be explored in the near future.

It is important to mention that the simulations reach a grand design quasi-steady state, although the position and pitch angle of the arms oscillate slightly around the above quoted values, and waves travel through the disk reflecting off the resonances and numerical boundaries.

It is quite noticeable the presence of an MHD instability at the position of corotation. Its seeds can already be seen as early as 1.5 Gyr, but it fully develops 2.5 Gyr into the run. After approximately 6 Gyr, the turbulence generated by the instability already spans all but the innermost disk regions. This instability appears to be quite robust; it is always present in the magnetized simulations, but absent in the pure HD simulations. More details about this phenomenon are provided in M. Martos contribution and in [10].

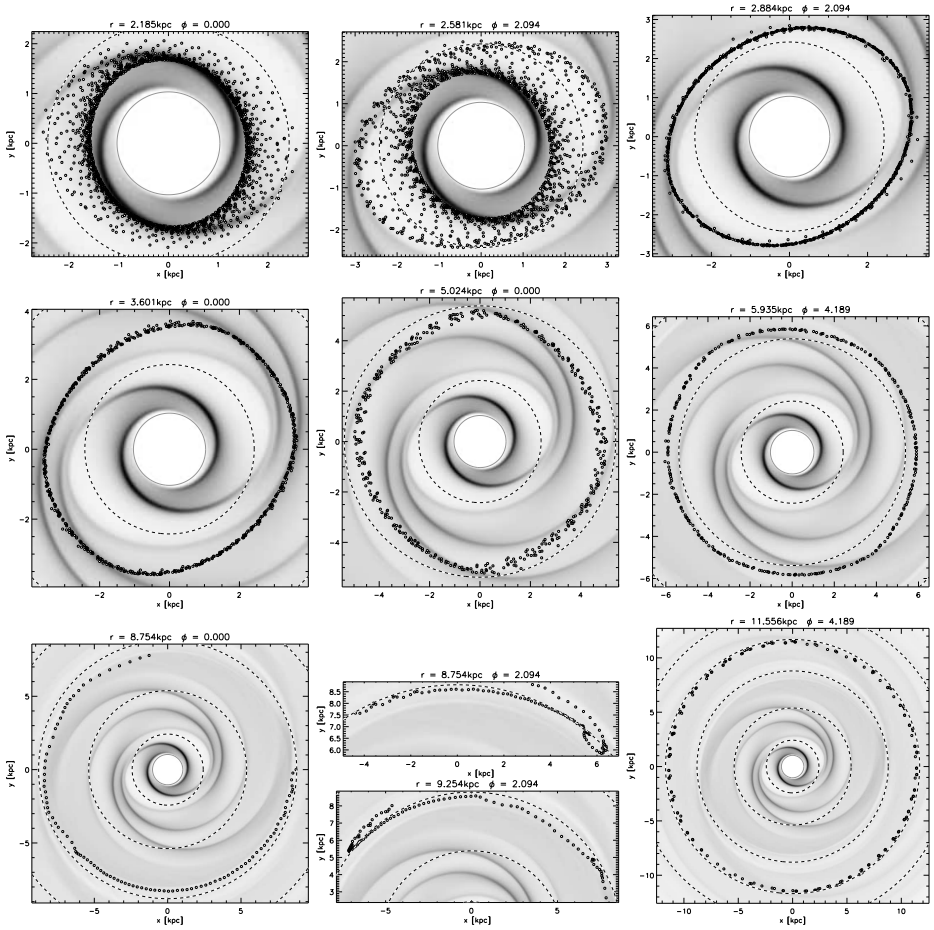

Fig. 1. Orbits of the gas in the simulation. Each panel is labeled with the initial position of the gas element, with angles measured counterclockwise starting from the positive x-axis. The dashed circles represent the position of the resonances (see text). The orbits are plotted on top of the density distribution averaged over 3 Gyr.

3 THE GASEOUS ORBITS

Since ZEUS is an Eulerian code, it does not directly provide the actual orbits the gas follows during the evolution of the disk. Nevertheless, they can be reconstructed by performing a Runge-Kutta integration of the velocity data, interpolating in time between data dumps. Figure 1 presents several orbits of the gas integrated over 3 Gyr of evolution.

Several families of orbits, very similar to the principal family orbits obtained in stellar dynamics, are readily distinguishable, with transitions

from one family to another near the position of the resonances. For example, the orbits integrated from initial position near or internal to the ILR [e.g. $(r/\,\mathrm{kpc}, \phi) = (2.185, 0.000)$] rapidly spiral inwards and settle in the ring/arm+spur structure at $r \approx 1.5\,\mathrm{kpc}$. Outside the ILR, [e.g. $(r/\,\mathrm{kpc}, \phi) = (2.884, 2.094)$], orbits tightly follow a simple oval, although they show some dispersion. The oval orbit becomes squarish as we move outwards [$(3.601, 0.000)$ orbit], with the dispersion steadily increasing as one pair of arms weakens [$(5.024, 0.000)$ orbit], until we reach the 4:1 resonance and oval (but cuspy) orbits are recovered [$(5.935, 4.189)$ orbit]. Banana-shaped orbits are frequently observed near the corotation radius, as expected. Outside corotation, orbits are nearly circular with deviations from the initial radius smaller than 0.5 kpc, even if the spiral perturbation is still present (it dies off at $r = 12\,\mathrm{kpc}$). Of course, since the gas velocity and density equations are solved simultaneously by ZEUS, the orbital shapes support the gaseous structures, namely the spiral arms, spurs and low density regions.

Sometimes we observe the gas moving from one orbital family to another. For example, the $(2.581, 2.094)$ orbit starts as an oval, but later spirals in. The turbulence generated by the corotation instability makes somewhat unpredictable which orbital family will be followed by the gas near corotation, as it may be pushed away [$(8.754, 0.000)$ orbit], trapped at corotation [$(8.754, 2.094)$], or brought across and then pushed away [$(9.254, 2.094)$].

Although these orbital behavior is similar to that observed in stellar dynamics [4], we are able point out a couple of differences. First, although the simulations are close to a steady state, orbits that do not close on themselves should be allowed since the gas keeps falling inwards. And second, we do not observe orbits other than the corresponding to the central family of periodic orbits of the stellar case.

References

1. M. Martos, X. Hernández, M. Yáñez, E. Moreno & B. Pichardo: MNRAS **350**, L47 (2004)
2. C. Allen & A. Santillán: Rev. Mex. Astron. Astrofis. **22**, 255 (1991)
3. B. Pichardo, M. Martos, E. Moreno & J. Espresate: ApJ **582**, 230 (2003)
4. G. Contopoulos & P. Grosbøl: A&A **155**, 11 (1986)
5. G. Contopoulos & P. Grosbøl: A&A **197**, 83 (1986)
6. R. Drimmel & D. Spergel: ApJ **556**, 181 (2001)
7. J. M. Stone & M. L. Norman: ApJS **80**, 753 (1992)
8. J. M. Stone & M. L. Norman: ApJS **80**, 791 (1992)
9. P. A. Patsis, N. Hiotelis, G. Contopoulos & P. Grosbøl: A&A **286**, 46 (1994)
10. M. Martos: *submitted*